RSC Advances

PAPER

View Article Online
View Journal | View Issue

Cite this: *RSC Adv.*, 2026, **16**, 13381

Coumarin thiazole-derived Schiff base copper complex: synthesis, characterization, and applications in the catalytic degradation of dyes, pearl millet seed germination for improved agricultural output and antioxidant assays

Neelam Sharma, Kanchan and Rahul Shrivastava *

In this work, we report the synthesis, characterization, catalytic degradation of dyes, and antioxidant scavenging assay of a coumarin thiazole-derived Schiff base (CTSB) copper complex and its impact on pearl millet seed germination. The coumarin thiazole Schiff base ligand was synthesized from diethylamino salicylaldehyde and a coumarin thiazole-based amine. The catalytic degradation of organic dyes using the synthesized coumarin thiazole-derived Schiff base (CTSB) copper complex exhibited 99.89% degradation of methylene blue within 35.0 seconds, while 94.22% of rhodamine B was degraded at room temperature within 3.0 minutes upon exposure to sunlight under optimum reaction conditions. Moreover, 92.88% of Congo red and 70.65% of methyl orange were degraded within 20.0 minutes and 12.0 minutes, respectively, at room temperature upon exposure to sunlight; similar percentages of degradation were obtained within 12.0 minutes and 4.0 minutes, respectively, when they were exposed to ultraviolet light. Additionally, the coumarin thiazole-derived Schiff base (CTSB) copper complex exhibited outstanding antioxidant activity (90.59%) against DPPH assays. Further, the effect of the developed CTSB-copper complex on seed germination was examined on hybrid pearl millet seeds. Methylene blue and methyl orange exhibited approximately 30% and 17% reduction in seed germination, respectively, in comparison to the control. The treatment with the CTSB-copper complex neutralized the effect of methylene blue and methyl orange dyes on the percentage germination of hybrid pearl millet seeds. The present findings highlight the potential of the CTSB-copper complex as a sustainable material for environmental remediation and for various applications in agriculture and biological sciences.

Received 27th October 2025
Accepted 10th February 2026

DOI: 10.1039/d5ra08232c

rsc.li/rsc-advances

1. Introduction

Rapid industrialization, improper treatment of effluents, human excreta, domestic wastages, untreated sewage and unscientific disposal of industrial waste have increased environmental pollution, especially water and air pollution.[1] Water pollution is usually caused by contaminated effluents from dying, textiles, plastic, paint and pharmaceutical industries, and a major part of water pollution is contributed by textiles and dye industries.[2] It is estimated that up to 20% of total dyes utilized in the dyeing process and textile production are released into water bodies without any pre-treatment.[3,4] Synthetic dyes are generally complex organic/inorganic moieties and are sparsely biodegradable in nature, causing hazardous effects on the environment and living organisms. Moreover, dye-contaminated effluents pose severe ecological problems because of their harmful long-lasting color, imposing excessive COD load on water, which hampers biodiversity in aquatic ecosystems.[5] Among various categories of synthetic dyes, azo dyes are non-biodegradable, recalcitrant, colourful and persistent in nature. Owing to their unpredictable and xenobiotic nature, azo dyes cause long-term hazardous effects on life by inducing extreme variations in dissolved oxygen, pH, chemical oxygen demand and dissolved toxic salts. In azo dye-polluted water, light penetration efficiency inside the aquatic system is significantly decreased, which severely affects the water ecosystem. Further, toxic substances present in azo dyes are responsible for severe health issues, like sporadic disorder, hypertension, cancer, and cramps with prolonged effects, in human beings.[6–8] Considering the detrimental effects on human health and aquatic ecosystems, the treatment of dye-contaminated textile effluents is a warranted and critical environmental challenge. Several physicochemical processes are used for the treatment of dye-contaminated industrial effluents such as coagulation, flocculation, filtration, precipitation, flotation, chlorination, adsorption, oxidation, ion exchange,

Department of Chemistry, Manipal University Jaipur, VPO-Dehmi-Kalan, Off Jaipur-Ajmer Express Way, Jaipur, Rajasthan, 303007, India. E-mail: chem.rahul@gmail.com

reverse osmosis, ozonation, Fenton oxidation, bleaching and aerobic/anaerobic degradation processes. Although most of these processes have several advantages, they also have drawbacks such as high capital costs, low removal efficiencies, and production of large amounts of sludge as byproducts, which need additional deposition or treatment.[9–12] Microbial processes are another choice for mineralization of dyes, but its complex biological process slows down the rate of degradation, which limits its utility in industrial scale.[13]

Transition metals have different coordination numbers and possess variable oxidations states, making them capable of forming stable transition metal complexes with unique physical, chemical and biological properties and can be utilized as versatile catalysts in various chemical transformations.[14] Schiff bases are well-known efficient auxiliary organic ligands because of their ease of synthesis, affordability and chemical and thermal stability.[15,16] The exclusive biological and pharmaceutical activities, superior catalytic properties, medicinal value and versatile industrial applications of Schiff bases have encouraged researchers worldwide to synthesize transition metal complexes of various types of Schiff base ligands and use them for different applications.[17–24] Despite their several advantages, the toxicity of transition metal complexes of Schiff base ligands is an important criterion in the evaluation of their suitability for a broad spectrum of applications. It was observed that in several cases, the toxicity of these complexes primarily depends on the nature of the Schiff base and the metal ions used in the formation of the complex. Copper ions are known to regulate various biological functions in the living system. It is reported that copper complexes of Schiff base moieties can penetrate through the bacterial cell wall because of their lipophilic nature compared to copper ions and Schiff base moieties, established by comparison of the charge distribution between metal ions and Schiff base ligands.[25,26] Additionally, copper ions can form stable metal complexes with Schiff base ligands and this stabilization result in a substantial reduction in toxicity over free metal ions of copper chlorides for living organisms because of lowering their capacity to engage in damaging oxidative processes.[27]

Coumarin (2*H*-pyran-2-one) contains an α-pyrone ring and fused benzene and is classified as a fundamental moiety of multiple heterocyclic families. The possibilities of various structural substitutions on the coumarin scaffold make them viable for biological, medicinal and pharmaceutical applications.[28–32] Derivatives of coumarin exhibit numerous biological activities such as anticoagulant, anti-oxidation, anthelmintic, antibacterial, anti-cancer, anti-microbial, anti-inflammatory, anti-depressant, hypothermal, anti-Alzheimer, and vasodilatory activities.[33] Thiazole is another important heterocyclic moiety, with demonstrated potent applications as fungicides, sulfur drugs, dyes, biocides, chemical reaction stimulators and used as anti-bacterial, analgesics, antioxidants, anti-allergic, anti-cancer, anti-hypertensive, anti-malarial, anti-inflammatory, anti-psychotic, and HIV-1 reverse transcriptase inhibitors.[34]

Azo dyes such as rhodamine B (Rh B), methyl orange (MO), Congo red (CR), and methylene blue (MB) are extensively utilized in dying, paper, textile and pharmaceutical industries (Fig. 1). They are non-biodegradable and persistent in nature, hence mineralization of these dyes by reduction with sodium borohydride using a suitable catalyst is an attractive, convenient and environmentally benign method.[35] An in-depth literature survey revealed that Schiff base metal complexes are utilized in the mineralization of azo dyes.[36,39] Considering the degradation ability of Schiff base metal complexes, it was envisaged that the complexation of copper metal ion with Schiff bases may be an efficient and sustainable strategy for the catalytic reduction of azo dyes without producing secondary pollutants.[37,38]

In this report, we present the synthesis, characterization and applications of a new coumarin thiazole-derived Schiff base copper complex (CTSB-copper complex). The ligand, coumarin thiazole-derived Schiff base (CTSB), was synthesized from amino-thiazole coumarin and *N*,*N*-diethylamino salicylaldehyde using a facile synthetic method. The newly developed coumarin thiazole Schiff base (CTSB) possesses a coumarin-thiazole scaffold connected to an *N*,*N*-diethylamino-substituted salicylaldehyde *via* an imine bridge. The design of CTSB ligands provide unique hetero-tridentate coordination environment around the copper ion by extending the π-conjugated system with multiple donor sites (O, N, and S). This combination significantly improves chelation and electron transfer and stabilizes the metal centre, facilitating effective light-absorbing capacity and remarkably quick catalytic dye reduction under mild conditions. The copper complexes of coumarin thiazole-derived Schiff base were evaluated for reductive degradation of commonly used dyes, such as methylene blue, methyl orange, rhodamine B and Congo red, using $NaBH_4$ as reductant, thereby emphasizing their ability as an effective catalyst. In another noteworthy application, the effect of metal complexes on the germination of pearl millets was examined. The antioxidant properties of the reported metal complex were also evaluated against DPPH.

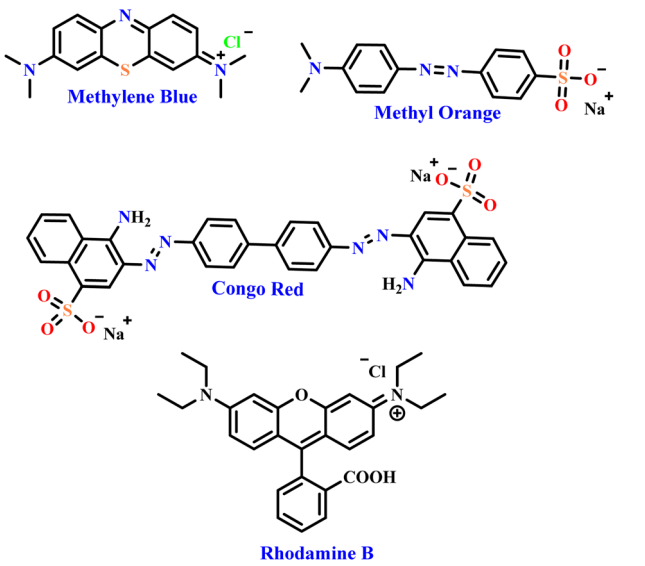

Fig. 1 Some commonly used azo dyes.

2. Experimental section

2.1. Materials and methods

Analytical grade reagents were used during the synthetic procedure of coumarin thiazole-derived Schiff base. Methylene blue, rhodamine B, methyl orange, Congo red and DPPH were purchased from HI-media, and experiments were carried out in ethanol solvent. Pearl millet seeds (RHB-234 improved) were procured from the RARI (Rajasthan Agriculture Research Institute), Durgapura, Jaipur, India. The progress of the reaction and the purity of the product were evaluated using thin layer chromatography. KBr pellets were used for recording FT-IR spectra on a JASCO FT/IR 4600 spectrophotometer. The absorbance spectra were obtained using a UV-VIS spectrophotometer (Shimadzu UV-2600). A rectangular, closed, light-shielded photoreactor (23 cm × 36.5 cm × 29.5 cm; height × width × length) was used for the dye degradation studies. UV lamps (Osram puritec HNS 8W germicidal Hg lamp) provide uniform irradiation inside the chamber, while the outer housing prevents interference from external light (Fig. S6, SI). The lamp emits UV radiation at 254 nm wavelength, and the intensity of the UV light was found to be 330 lux using LX-101A, HTCTM Lux meter. The intensity of sunlight was measured at 30 min intervals from 1.0 p.m. to 3.0 p.m. and was found to be 50 700 lux.

2.2. Dye degradation studies

The catalytic activity of the synthesized coumarin thiazole-derived Schiff base copper complex was evaluated for the degradation of four commonly used organic dyes, methylene blue, methyl orange, Congo red and rhodamine B, in aqueous medium. Sodium borohydride ($NaBH_4$) was used as a reducing agent to perform the catalytic degradation of dyes. The dye degradation studies were carried out with specific amounts of coumarin thiazole-derived Schiff base (CTSB) copper complex as a catalyst and sodium borohydride as a reducing agent under exposure to sunlight and UV-visible light. To examine the effect of sodium borohydride on the degradation of dyes, a negative control experiment was performed with $NaBH_4$ without using the synthesized CTSB-copper complex as a catalytic agent. In dye degradation studies, various amounts of the CTSB-copper complex, such as 1.0 mg, 3.0 mg and 5.0 mg, were added to 20.0 mL of aqueous solution of dyes (methylene blue, methyl orange, Congo red and rhodamine B) and 1.0 mL of freshly prepared 0.25 M sodium borohydride solution. The reaction mixture was stirred for different time intervals like 5.0, 10.0, 15.0 and 30.0 minutes, and the filtrate was collected for UV-visible spectroscopy analysis.

2.3. Seed germination studies

To monitor the effect of methylene blue (MB) and methylene orange (MO) dyes on seed germination, hybrid pearl millet seed was selected, along with a solution of 100 ppm of both dyes, MB and MO, was used for studies. The hybrid pearl millet seeds were sterilized with 0.1% NaOCl solution for a few minutes and then rinsed three times with Milli-Q water. The seed germination experiment was performed *via* the paper towel method in Petri dishes. In these experiments, fifteen seeds of pearl millet were taken in each Petri dish and treated with 100 ppm of the MB and MO dye solution. Similarly, another fifteen seeds were taken in a Petri dish and treated with 100 ppm of the dye solution and 150 ppm solution of the synthesized CTSB copper complex. On the other hand, a priming test was conducted with 150 ppm doses of the CTSB copper complex, only using the same type of pearl millet seed. A plant growth chamber was used to incubate each Petri dish for five days at 27 °C. The experiment was carried out in the dark and each treatment was assessed using three replicates. The percentage germination and physiological parameters, such as root length and shoot length, of fifteen randomly selected plants of each setup of pearl millet seedlings were recorded after a 5 day incubation period. The percentage germination was recorded by the following formula:

$$\text{Germination\%} = \left(\frac{\text{Germinated seeds}}{\text{Total seeds}}\right) \times 100$$

2.4. Antioxidant study

The scavenging capability of 2,2-diphenyl-1-picrylhydrazyl (DPPH) was monitored using previously reported methods.[40] Different doses of coumarin-thiazole Schiff base (CTSB) copper complex (0.5 to 2.5 mg mL^{-1} in MeOH) were used, and aliquots of the complex were added to 3.0 mL of 0.1 mM DPPH in methanolic solution. The resultant solutions were kept for half an hour at 27 °C in darkness; subsequently, the absorption spectra of the resultant mixture were recorded at 517 nm using UV-visible spectroscopy. As a positive control, ascorbic acid and methanol were used as a blank in this experiment. The following equation was used to determine the percentage inhibition antioxidant property:

$$\%\ \text{Inhibition} = \left(\frac{A_{\text{control}} - A_{\text{sample}}}{A_{\text{control}}}\right) \times 100$$

where A_{control} is the absorbance of DPPH (without compound) and A_{sample} is the absorbance of DPPH with the complex.

2.5. Statistical analysis

All experiments were performed with mean ± standard deviation (SD) in triplicate. Data on mechanical characteristics were analyzed using ANOVA in SPSS (IBM, SPSS Statistical software, 29.0). The *p*-value was less than 0.05, and the differences were confirmed using Duncan's test.

3. Results and discussion

3.1. Synthesis and characterization of the coumarin thiazole-derived Schiff base ligand and its copper complex

The coumarin thiazole-derived Schiff base ligand was obtained starting from 3-acetylcoumarin in a facile five-step synthetic procedure, as depicted in Scheme 1. The starting material, 3-acetyl coumarin, was synthesized by the reaction of ethyl acetoacetate (2.48 mL) with salicylaldehyde (16.3 mmol) using a catalytic amount of piperidine in ethanol (4.0 mL) at room temperature. In the next step, 3-acetylcoumarin (1.06 mmol)

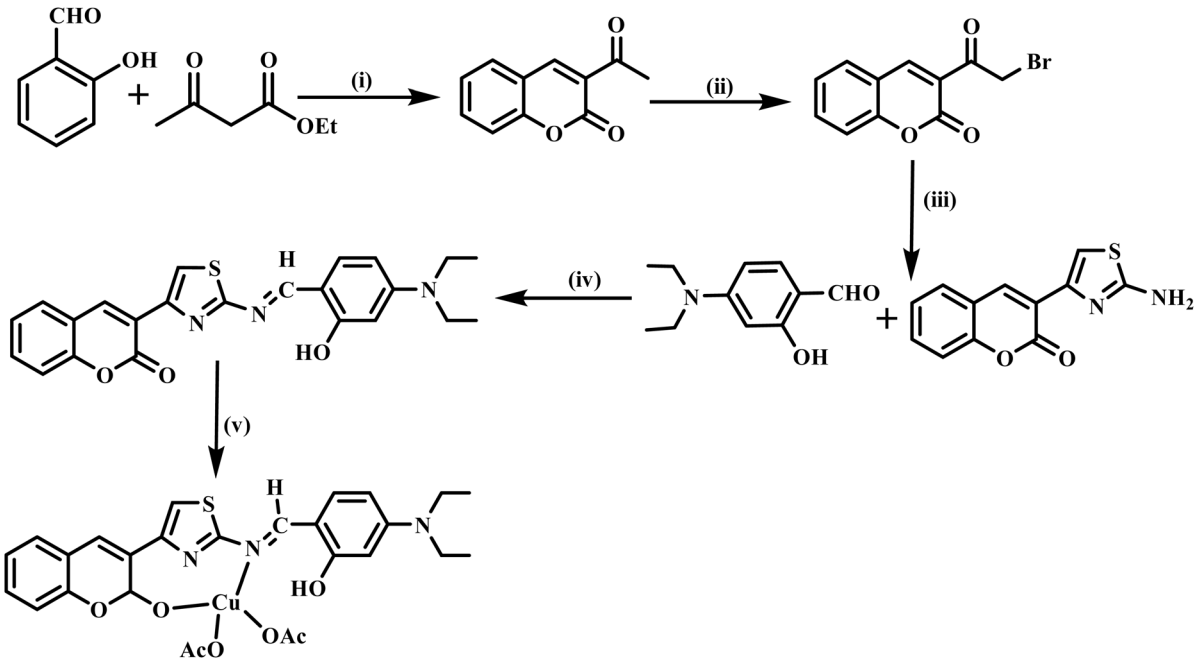

Scheme 1 Synthesis pathway of the coumarin thiazole-derived Schiff base ligand (CTSB) and its copper metal complex. Conditions: (i) piperdine, ethanol, RT; (ii) Br_2, dry $CHCl_3$, 0 °C, 3.0 h; (iii) thiourea, ethanol, reflux, 80 °C; (iv) ethanol, reflux, 8.0 h; and (v) $Cu(OAc)_2$, reflux.

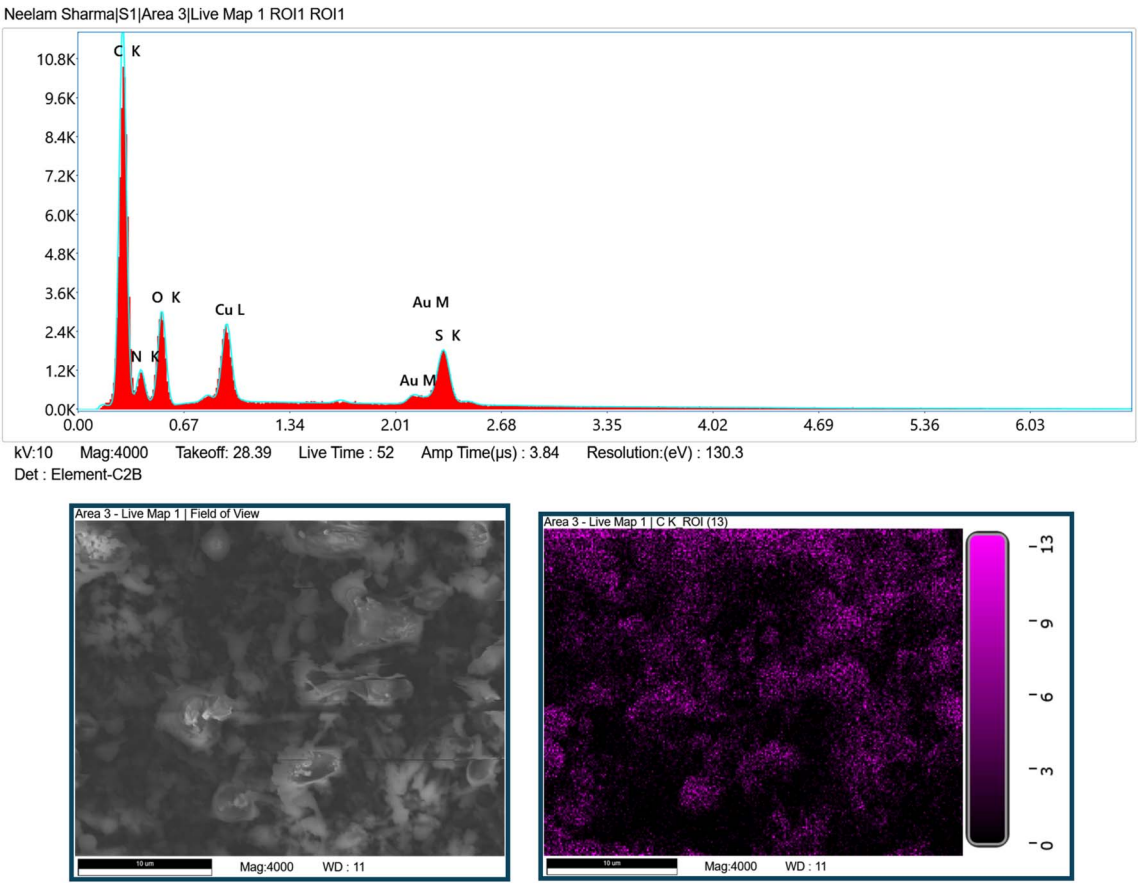

Fig. 2 EDX spectra and mapping of the coumarin thiazole-derived Schiff base copper complex (CTSB-Cu).

was reacted with 1.3 eq. of bromine in chloroform at 0 °C for 3.0 h to provide 3-(bromoacetyl)-2*H*-chromen-2-one (5) in 90% yield. Further, 3-(2-aminothiazol-4-yl)-2*H*-chromen-2-one was synthesized from the reaction between thiourea (0.38 mmol) and 3-(bromoacetyl)-2*H*-chromen-2-one (0.38 mmol) in ethanol (6.0 mL) at 80 °C for 4–5 h.[41] The coumarin thiazole-derived Schiff base ligand was afforded by refluxing the synthesized intermediates 3-(2-aminothiazol-4-yl)-2*H*-chromen-2-one (0.21 mmol) with *N*,*N*-diethylamino salicylaldehyde (0.21 mmol) in ethanol (10.0 mL) for 8.0 h. The target coumarin thiazole derived from the Schiff base copper complex was synthesized by overnight refluxing of copper acetate with the synthesized Schiff-base ligand (1 : 1 molar ratio) in ethanol (10–12.0 mL) to give a green-brown precipitate, which was filtered and washed with cold ethanol and purified with diethyl ether. The synthesized copper complex was dried under vacuum at 70 °C, giving a green-brown colored powder with 85% yield.

The structures of coumarin thiazole-derived Schiff base (CTSB) and its copper complex were analyzed by XRD, EDX, TGA, CHN elemental analysis, nuclear magnetic resonance, FT-IR and mass spectrometry. The elemental analysis was performed to determine the presence of various elements in coumarin thiazole-derived Schiff base (CTSB) and its copper complex. The percentage ratios of carbon, hydrogen and nitrogen (C, H and N) were theoretically calculated for the CTSB-copper complex. The experimentally obtained values (C 53.75%; H 4.73%; N 6.89%) were aligned with the theoretically calculated values (C 53.86%; H 4.69%; N 6.98%). Furthermore, to investigate the successful metal complexation of the CTSB ligand and coordination of the Cu metal on the resulting CTSB-Cu complex, EDX mapping of CTSB-Cu was carried out, as shown in Fig. 2. The EDX analysis confirms the presence of carbon, nitrogen, oxygen, sulfur and copper in the synthesized metal complex.

The structures of coumarin thiazole derived Schiff base (CTSB) and its copper complex were initially analyzed by nuclear magnetic resonance, FT-IR and mass spectrometry (see Fig. S1–S3 in SI). The FT-IR spectra of the CTSB ligand and its copper complex are depicted in Fig. 3. The FT-IR spectrum of the CTSB ligand showed a peak at 3450 cm^{-1}, which was attributed to O–H stretching, whereas the peak at 3029 cm^{-1} was associated with aromatic C–H stretching. Similarly peaks at 1720 cm^{-1} and 1602 cm^{-1} were attributed to C=O stretching of the carbonyl group of the coumarin moiety and imine group (C=N) of the Schiff base, respectively, whereas the existence of the thiazole moiety was confirmed by the appearance of peaks at 783 cm^{-1} and 1137 cm^{-1}, assigned to C–S and C–N stretching.[29,42] The FT-IR spectrum of the copper complex of the CTSB ligand demonstrated a shift in the peak at 1602 cm^{-1}, and the appearance of a peak at 594 cm^{-1} indicated the coordination of the copper ion with the CTSB ligand oxygen and nitrogen atoms. These observations revealed the involvement of imine and carbonyl groups in complexation with the copper ion.

The electronic properties of the coumarin thiazole-derived Schiff base ligand (CTSB) and its copper complex were examined by UV-visible spectroscopy (Fig. 4). The UV-visible

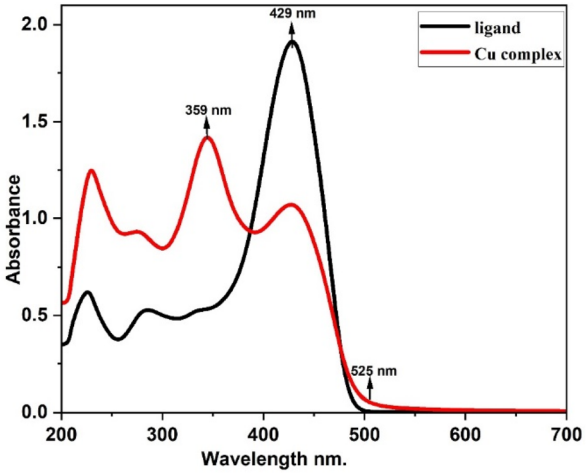

Fig. 4 UV-visible spectra of coumarin thiazole-derived Schiff base (CTSB) ligand and its copper complex.

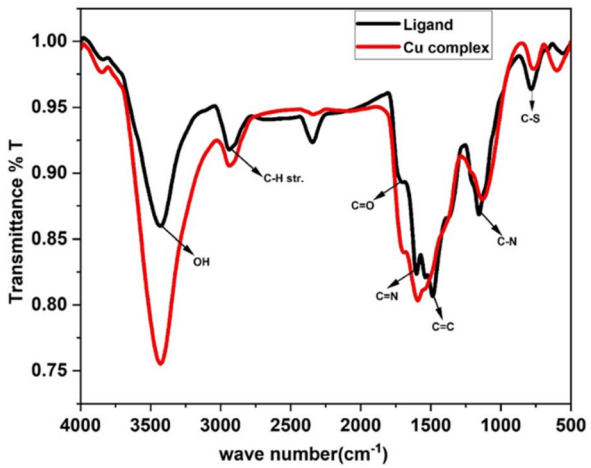

Fig. 3 FT-IR spectra of coumarin thiazole-derived Schiff base (CTSB) ligand and its copper complex.

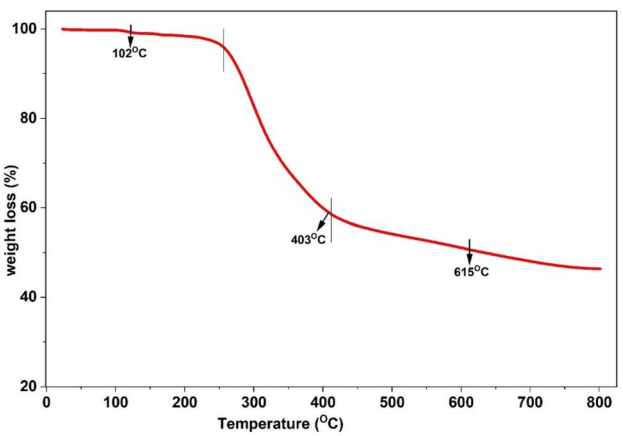

Fig. 5 TGA analysis of the coumarin thiazole-derived Schiff base copper complex.

spectrum of a 2.38×10^{-5} M solution of the synthesized CTSB ligand in acetonitrile exhibited a peak at 295 nm, along with sharp absorption bands at 429 nm. The peak at 295 nm was associated with the π–π* transition of the aromatic C=C group, whereas the sharp band at 429 nm was denoted as the n–π* transitions of the azomethine group. The UV-visible spectra of the copper complex of the CTSB ligand showed peaks at 295 nm, 359 nm and 429 nm. The new absorption peak at 359 nm in the copper complex of the CTSB ligand might be a consequence of charge transfer modulation from the metal to the ligand. However, minor variations in the position and intensity of other bands in the metal complex spectra, as compared to the CTSB ligand spectrum, are due to complexation of the copper ion with the coordination sites of the CTSB ligand. Moreover, an absorption band at 525 nm was observed because of the d–d transitions of metal ions.[43]

The TGA analysis of the CTSB-Cu complex is illustrated in Fig. 5. A slight weight loss of 1–2% is attributed to the dehydration of water molecules at 102 °C. The 42% weight loss obtained between 200–400 °C was ascribed to the degradation

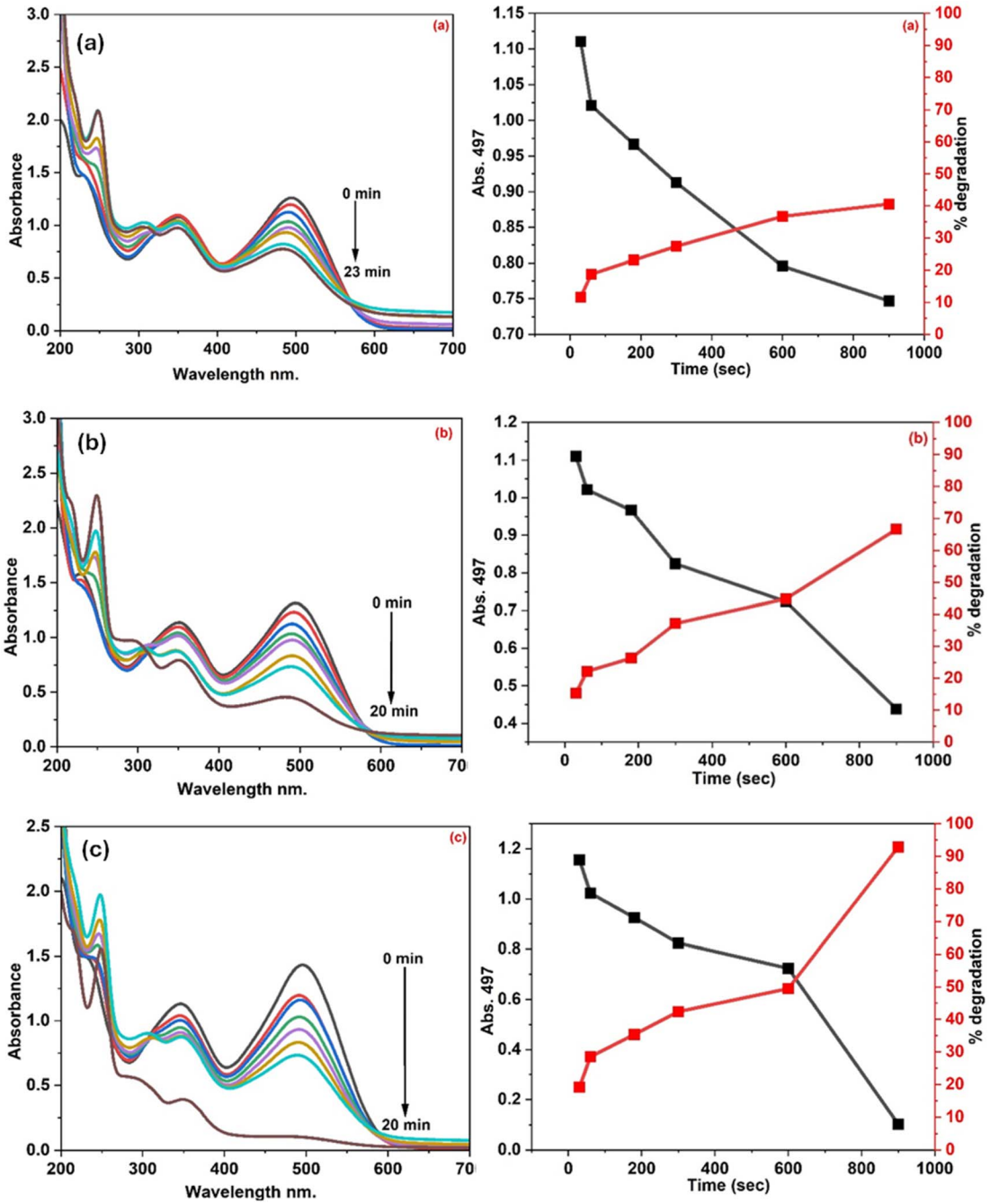

Fig. 6 UV-vis degradation spectrum of the Congo red (CR) dye using $NaBH_4$ and the CTSB-copper complex at various doses: (a) 1.0 mg, (b) 3.0 mg, and (c) 5.0 mg.

of the acetate unit and Schiff-base ligand. The 6–8% weight loss appeared at 400–800 °C due to the residual metal oxide. Further, the XRD spectra of coumarin thiazole-derived Schiff base (CTSB) ligand and its copper complex were recorded (Fig. S4, SI). The XRD spectrum of the CTSB ligand showed a peak at $2\theta = 24.9°$, indicating the formation of Schiff-base imine. The XRD pattern of coumarin thiazole-derived Schiff base (CTSB)-copper complex clearly demonstrated that the crystalline index of the Schiff base ligand CTSB at $2\theta = 24.9°$ shifted to $2\theta = 17.4°$ owing to the π–π conjugation between the metal ion and the ligand.[44]

3.2. Degradation studies of the CTSB-copper complex for methylene blue, methyl orange, Congo red and rhodamine dyes

The dye mineralization studies of the synthesized coumarin thiazole-derived Schiff base (CTSB)-copper complex were examined for methylene blue (MB), methyl orange (MO), Congo red (CR) and rhodamine B (Rh B) dyes using $NaBH_4$ as a reducing agent at room temperature in aqueous medium. The reducing ability of sodium borohydride towards the MB, MO, CR and RhB dyes without using the CTSB-copper complex was monitored by the treatment of 20.0 mL of the aqueous solution

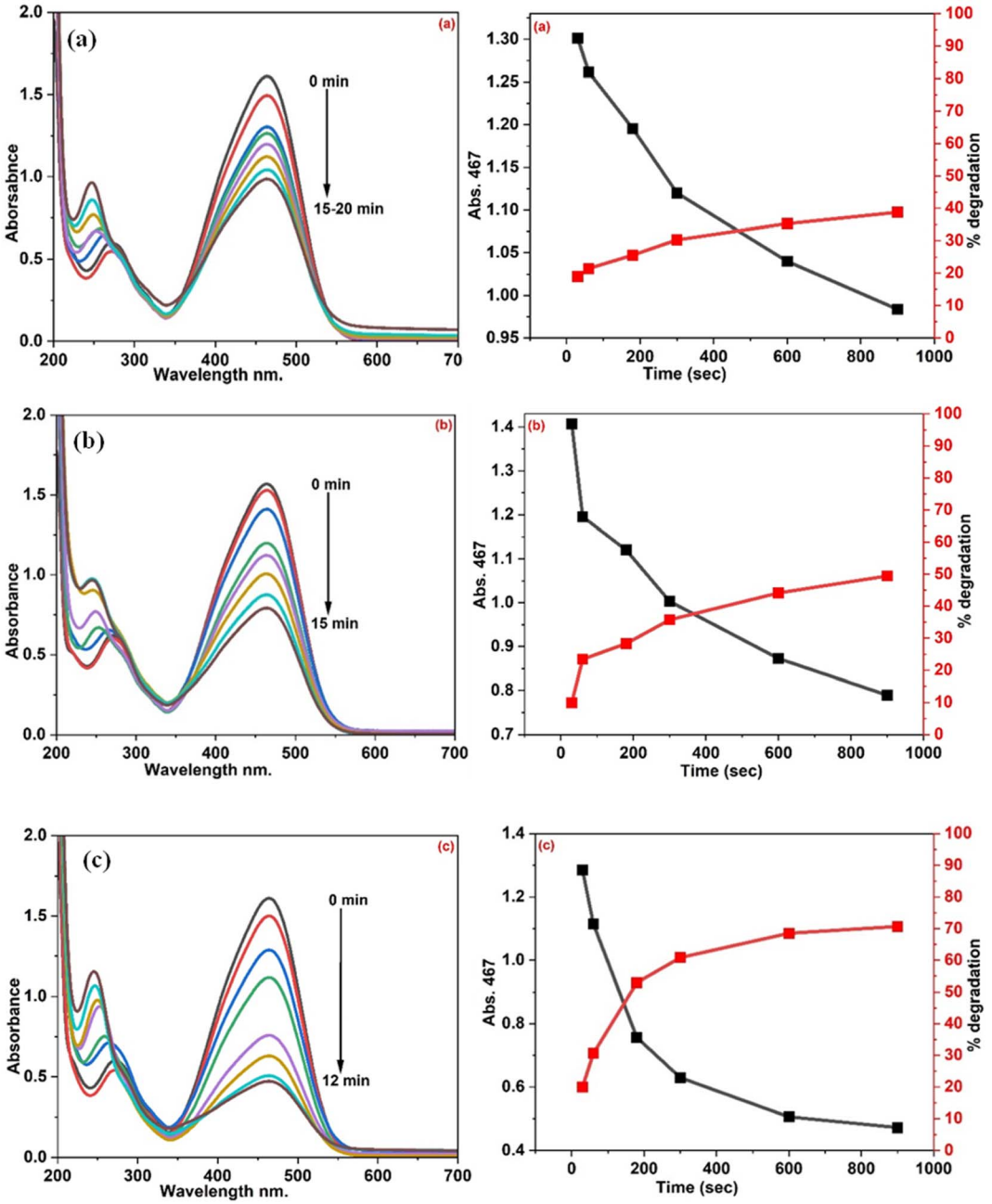

Fig. 7 UV-visible spectrum of the degradation of methyl orange (MO) dye using $NaBH_4$ and the CTSB-copper complex at various doses: (a) 1.0 mg, (b) 3.0 mg and (c) 5.0 mg.

of MB, MO, CR and RhB dyes (100 ppm) individually with $NaBH_4$ (1.0 mL; 0.25 M) at room temperature under solar light and UV-visible light for 30.0 minutes. The results revealed negligible degradation of the tested dyes without the CTSB-copper complex (Fig. S5, SI). Subsequently, separate aqueous solutions of MB, MO, CR and RhB dyes were treated with 5.0 mg of the coumarin thiazole-derived Schiff base ligand (CTSB) in the presence of $NaBH_4$ at room temperature. No reduction of dyes was recorded even after 30.0 minutes of treatment. Interestingly, decolorization of all four dyes (MB, MO, CR and RhB) was observed on the addition of the CTSB-copper complex in the presence $NaBH_4$ at room temperature, indicating the degradation of these dyes. Further, degradation reactions of MO, CR, MB and RhB dyes using $NaBH_4$ and the synthesized CTSB-copper complex were individually optimized in terms of time, catalyst dose, temperature and light irradiation parameters using UV-visible spectroscopy.

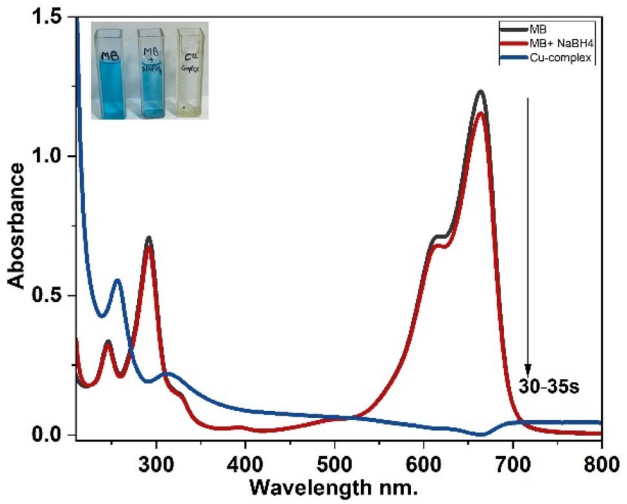

Fig. 8 UV-visible spectra of the degradation of methylene blue (MB) dye using $NaBH_4$ and CTSB-copper complex.

The absorption spectrum of a 5.49×10^{-5} M solution of Congo-red (CR) was recorded in aqueous solution. The absorption spectra exhibited an intense peak at 497 nm and a small peak at 350 nm, which was ascribed to the n–π* transition of the azo group and π–π* transition of aromatic rings, respectively. The degradation of the CR dye was evaluated with the CTSB-copper complex and $NaBH_4$ at various time periods (0 to 30.0 minutes) and various amounts of catalyst doses. It was observed that a negligible change was noticed in the peak at 497 nm in the absorption spectra of CR dyes without using the reported CTSB-copper complex, which indicated that the degradation process was negligible without the complex. On the addition of 10.0 mg of the CTSB-copper complex, the absorption peak at 497 nm of CR almost disappeared within 15.0 minutes at room temperature. Further, the catalyst dose was optimized by performing different sets of experiments using 1.0 mg, 3.0 mg, 5.0 mg and 10.0 mg CTSB-copper complex with $NaBH_4$ (1.0 mL; 0.25 M) at room temperature on exposure to sunlight. The degradation percentages of the CR dye were found to be 40.58%, 66.60% 92.88% and 92.78% within 20.0 minutes using 1.0 mg, 3.0 mg, 5.0 mg and 10.0 mg of the CTSB-copper complex at room temperature, respectively. The maximum degradation efficiency of CR was found to be 92.88% within 20.0 minutes using 5.0 mg of the CTSB-copper complex. A significant reduction in degradation (66.60%) was noted when 3.0 mg of the catalyst was used, whereas the use of 10.0 mg of the catalyst had no significant impact on degradation efficiency. These results indicated that the degradation of the CR dye depends upon the amount of the CTSB-copper complex since it increases the number of active sites on the catalyst surface, which enhanced the degradation process, as depicted in Fig. 6. After optimizing the amount of the CTSB-copper complex, we explored the minimum time for maximum degradation by carrying the degradation process for 45.0 minutes using 5.0 mg of the CTSB-copper complex with $NaBH_4$ (1.0 mL; 0.25 M) at room temperature under exposure to sunlight. The average percentages of degradation at different time intervals indicated that 20.0 minutes was the minimum time for maximum catalytic

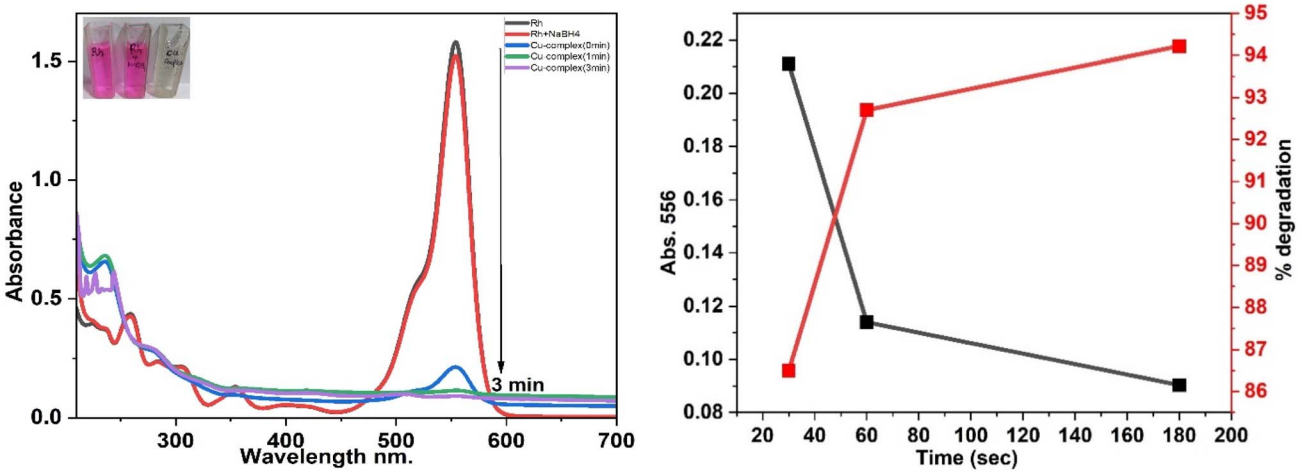

Fig. 9 UV-visible spectrum of degradation of rhodamine (Rh B) upon exposure to sunlight using $NaBH_4$ and CTSB-copper complex.

Table 1 Percentage degradation of the CR, MB, MO and RhB dyes upon exposure to ultraviolet and sunlight using the CTSB-copper complex

Dyes	CTSB-copper complex	Degradation (maximum)	Sunlight (minutes)	Ultraviolet light
Congo red	1.0 mg	40.58%	23.0 min	22.0 min
	3.0 mg	66.60%	20.0 min	18.0 min
	5.0 mg	92.88%	20.0 min	12.0 min
	10.0 mg	92.50%	30.0 min	30.0 min
Methyl orange	1.0 mg	38.77%	15–20 min	6.0 min
	3.0 mg	49.46%	15.0 min	5.0 min
	5.0 mg	70.65%	12.0 min	4.0 min
	10.0 mg	70.30%	15.0 min	15.0 min
Methylene blue	1.0 mg	99.89%	35 seconds	—
Rhodamine B	1.0 mg	94.22%	3.0 min	—

efficiency of the CTSB-copper complex at room temperature under sunlight. Moreover, a similar experiment was performed with an equal amount of the CTSB-copper complex on exposure to ultraviolet light, and 92.88% degradation of CR was achieved within 12.0 minutes. Interestingly, percentage degradation was not further enhanced even though the reaction was carried out for 30.0 minutes or when the amount of the complex was increased from 5.0 mg to 10.0 mg at room temperature.

In the case of methyl orange (MO), a 5.81×10^{-5} M aqueous solution of the MO dye exhibited an absorption band at 467 nm in UV-visible spectroscopy. The detailed investigation of absorption spectra clearly demonstrated that neither colour nor the absorbance peak at 467 nm was changed when the MO dye solution was treated with only sodium borohydride at room temperature on exposure to sunlight or ultraviolet light. The treatment of MO dyes with CTSB-copper complex and $NaBH_4$ under similar reaction conditions resulted in a decrease in the intensity of the absorption peak at 467 nm, along with decolouring of the MO dye solution. The degradation efficiency of the CTSB-copper complex for MO dyes was evaluated with different amounts and time intervals; therefore, different sets of experiments were performed with 1.0 mg, 3.0 mg, 5.0 mg and 10.0 mg CTSB-copper complex within a 20.0 minute time interval at room temperature under sunlight, as depicted in Fig. 7. The percentage degradation of the MO dye is 38.77%, 49.46%, 70.65% and 70.52% using 1.0 mg, 3.0 mg, 5.0 mg and 10.0 mg, respectively, within 15.0 minutes. It is notable that the degradation percentage was not enhanced or decreased by increasing either the amount of the complex or time of the reaction. Moreover, degradation of MO dyes was performed under exposure to ultraviolet light using an optimized amount of the CTSB-copper complex (3.0 mg). The results revealed that only 70.65% of the MO dye was degraded within 4–5 minutes, even though the experiment was extended for the next 45.0 minutes. The complete degradation of the MO dye was not achieved, even by increasing the dose of complexes or increasing the time under both sunlight and ultraviolet light irradiation.

Similarly, the degradation of methylene blue (1.78×10^{-5} M) was also monitored by the synthesized CTSB-copper complex under sunlight irradiation. The CTSB-copper complex completely degraded methylene blue dyes within 30–35 seconds using only 1.0 mg of the CTSB-copper complex, indicating that the reported complex is most effective for the degradation of MB dye among the four tested dyes (Fig. 8). Similarly, a 1.0 mg dose of the CTSB-copper complex initiated the degradation of rhodamine B dye (1.19×10^{-5} M) and after 45–50 s, decolorization was observed and around 94.22% rhodamine B dye degraded within 3.0 min under exposure to sunlight, as shown in Fig. 9.

The results of experimental data for the degradation of dyes using the CTSB-copper catalyst are tabulated in Table 1 based on the complex dose, average time required, and percentage degradation upon irradiation with sunlight and ultraviolet light.

Further, reaction kinetics studies for the degradation of CR, MO, RhB and MB dyes using the developed CTSB-Cu-complex were carried out. The reduction rates followed the pseudo-first order kinetics, as presented in eqn (1):

$$\ln C_t = \ln C_0 - k_{obs} \times t \quad (1)$$

where t is the reaction time, C_t is the concentration of the dye solution at time t and C_0 is the concentration of the dye solution at zero-time, k is the pseudo first order rate-constant. The rate constant k (min^{-1}) was determined from the slope of the $\ln(C_t/C_0)$ *vs.* time plot (Fig. 10). The rate constant values, which are calculated from the pseudo first order plot, are tabulated in Table 2.

The degradation of dyes utilizing $NaBH_4$ follows pseudo-first-order kinetics because of the excess concentration of $NaBH_4$. It was presumed that dissociation of sodium borohydride generates BH_4^{-1} and Na^+ ions and transfers the hydride ion to the CTSB-copper complex, which results in the formation of Cu-hydride bonds. The dyes capture hydrogen and electrons from the Cu-hydride complex, resulting in the reduction of functional groups.[45,46]

3.3. Radical scavenging activity

The antioxidant assay was carried out by *in vitro* radical scavenging activity of the synthesized coumarin-thiazole Schiff base copper complex using the DPPH (2,2-diphenyl-1-picrylhydrazyl) method. The dark purple-colored methanolic solution of DPPH exhibited an absorption peak at 517 nm owing to the presence of unpaired electrons/free radicals in the solution at room

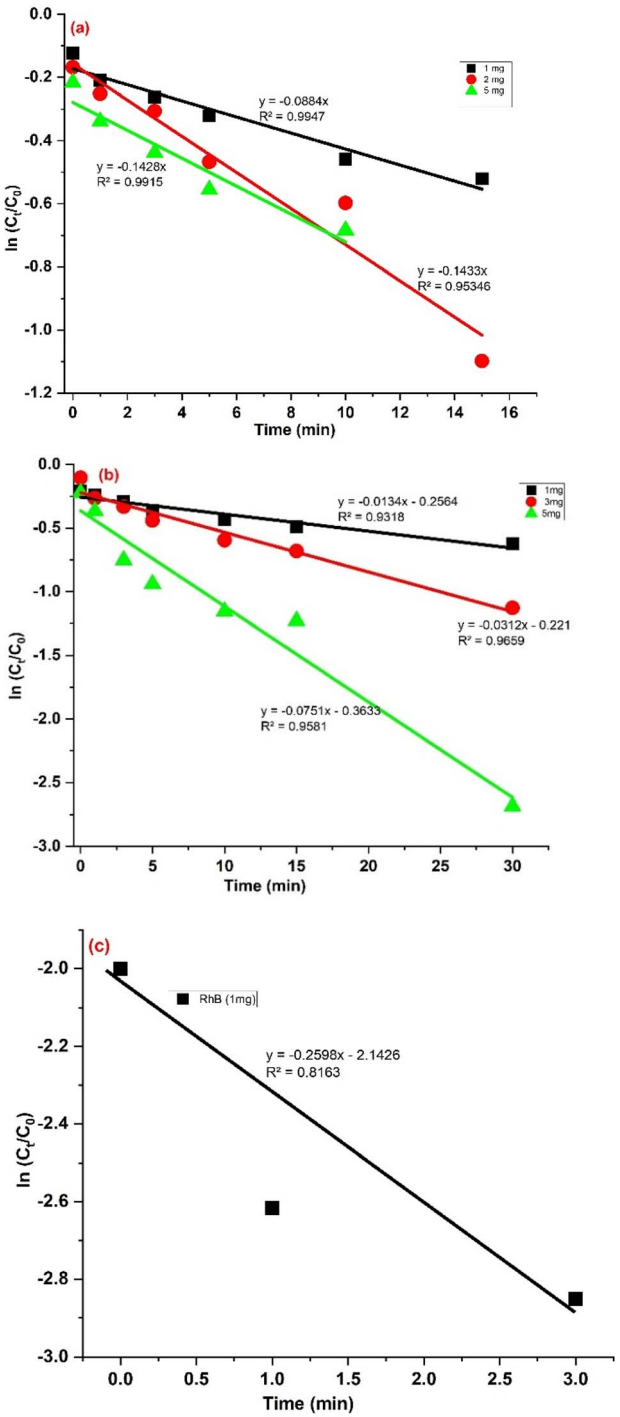

Fig. 10 Experimental degradation data with the pseudo first order kinetics model: (a) CR, (b) MO, and (c) RhB.

temperature. The absorption peak at 517 nm was decreased, along with the decoloring of the methanolic solution of DPPH in the dark, when the unpaired electron becomes paired off with respect to the number of electrons donated by antioxidant molecules or complexes. The noticeable changes in the intensity of absorbance by neutralization of free radicals could be extensively utilized to investigate the free radical scavenger

Table 2 Rate constant values of the CR, MO, RhB and MB dyes

Dyes	Conc. of dyes (initial)	Amount of the CTSB-Cu complex	Rate constant
Congo red	5.49×10^{-5} M	1.0 mg	0.02542 min^{-1}
	5.49×10^{-5} M	3.0 mg	0.05730 min^{-1}
	5.49×10^{-5} M	5.0 mg	0. 04431 min^{-1}
Methyl orange	5.81×10^{-5} M	1.0 mg	0.01339 min^{-1}
	5.81×10^{-5} M	3.0 mg	0.03123 min^{-1}
	5.81×10^{-5} M	5.0 mg	0.07511 min^{-1}
Rhodamine B	1.19×10^{-5} M	1.0 mg	0.25979 min^{-1}
Methylene blue	1.78×10^{-5} M	1.0 mg	0.19596 s^{-1}

Table 3 Effects of varying the amount of the CTSB-copper complex on the seed germination, shoot length and root length of pearl millet[a]

Treatments	Germination in %	Root length (cm)	Shoot length (cm)
Control	80.00%	8.83 ± 0.63^{a}	6.02 ± 0.45^{a}
50 ppm	79.62%	8.64 ± 0.81^{a}	5.93 ± 0.68^{a}
100 ppm	77.26%	8.33 ± 0.55^{a}	5.83 ± 0.40^{a}
150 ppm	78.86%	8.20 ± 0.73^{a}	5.83 ± 0.57^{a}

[a] Duncan's test ($P \leq 0.05$) was utilized to determine the statistical significance. The resulting data were reported as mean values along with relevant standard deviation.

capability of the tested molecules. Hence, a decrease in intensity of the absorbance peak indicates high antioxidant activity of the tested complex. The methanolic DPPH solution containing the synthesized coumarin-thiazole Schiff base (CTSB) copper complex exhibited a gradual decrease in the intensity of the absorption peak at 517 nm and a color change at room temperature in the dark because the CTSB copper complex donates electrons to DPPH free radicals and neutralizes them. The results of absorption studies revealed that the percentage inhibition was increased as the dose of the CTSB-copper complex increased, indicating that the antioxidant property was dependent on the loading dose of the complex. The maximum inhibition percentage was achieved as 90.59% at 2.5 mg mL^{-1} dose of the reported complex, as depicted in Fig. 11. All these findings clearly demonstrated that the synthesized coumarin-thiazole Schiff base copper complex has excellent antioxidant capacity. The CTSB-copper complex was found to be most potent with a 0.560 mg mL^{-1} IC_{50} value.

3.4. Effect of methylene blue, methyl orange and CTSB-copper metal complex on the germination of pearl millet (*Pennisetum glaucum*) seeds and other physiological features

It is observed that in the proximity of textile and dye processing industries, germination of seeds is severely affected because the dye-containing effluents are directly discharged into nearby land without pretreatment. This study demonstrated the extraordinary efficiency of CTSB-copper complex in the enhancement in seed germination since the mineralization capability of this complex for dyes offer valuable remedies for

Table 4 Effect of the methylene blue (MB) and methyl orange (MO) dyes on the seed germination, shoot length and root length of pearl millet[a]

Treatments	Seed germination (in %)	Exposure time (10 minutes)		Exposure time (20 minutes)	
		Shoot length (cm)	Root length (cm)	Shoot length (cm)	Root length (cm)
Control	80.00%	4.60 ± 0.38[a]	8.02 ± 0.35[a]	6.35 ± 0.28[a]	8.8 ± 0.23[a]
MB (100 ppm)	50.00%	1.38 ± 0.54[a]	2.15 ± 0.41[a]	2.3 ± 0.46[a]	3.04 ± 0.36[a]
MO (100 ppm)	63.33%	2.2 ± 0.44[a]	2.89 ± 0.56[a]	2.8 ± 0.41[a]	3.8 ± 0.47[a]

[a] Duncan's test ($P \leq 0.05$) was utilized to determine the statistical significance. The resulting data were reported as mean values along with relevant standard deviation.

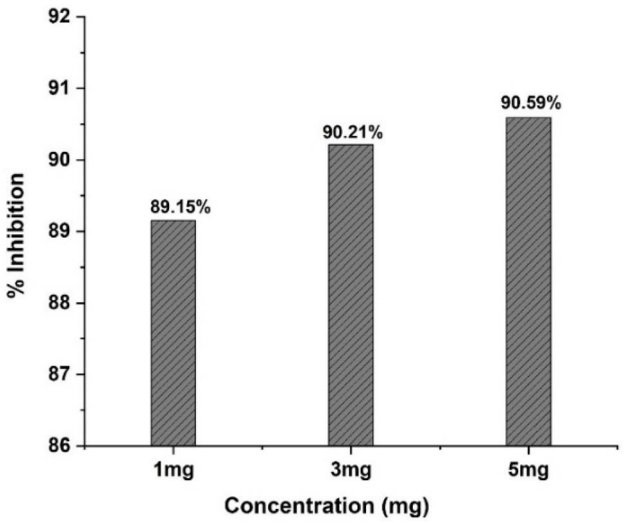

Fig. 11 Percentage inhibition of DPPH *via* the CTSB-copper metal complex at different concentrations.

environmental protection. In this study, initially, we evaluated the impact of the CTSB copper complex on the germination of pearl millet seeds. Therefore, treatment with different concentrations of the CTSB-copper complex (50, 100 and 150 ppm) was utilized to monitor pearl millet seed germination, shoot length and root length. The results revealed no impact of CTSB-copper complexes on percentage germination, shoot length and root length of pearl millet seeds was recorded in comparison to the control, as depicted in Table 3.

The percentage germination of pearl millet seeds and other physiological features, such as shoot length and root length, were also evaluated using MB and MO dyes and CTSB-complex-treated MO and MB dyes to determine how they affect pearl millet seed germination. Therefore, pearl millet seeds were treated with 100 ppm concentrations of MB and MO dyes. It was found that pearl millet seeds treated with 100 ppm methyl orange significantly decreased percentage germination, root length and shoot length compared with the control, as depicted in Table 3. Similarly, treatment with 100 ppm methylene blue dye decreases 30% of seed germination, whereas ~70% and ~73% of shoot length and root length, respectively, when exposed for 10.0 minutes (Table 4).

In contrast, in the case of pearl millet seeds treated with a solution of 100 ppm methyl orange or methylene blue dye and 150 ppm CTSB-copper complex, a significant enhancement in percentage germination, shoot length and root length was recorded, as shown in Fig. 12, which is similar to the control.

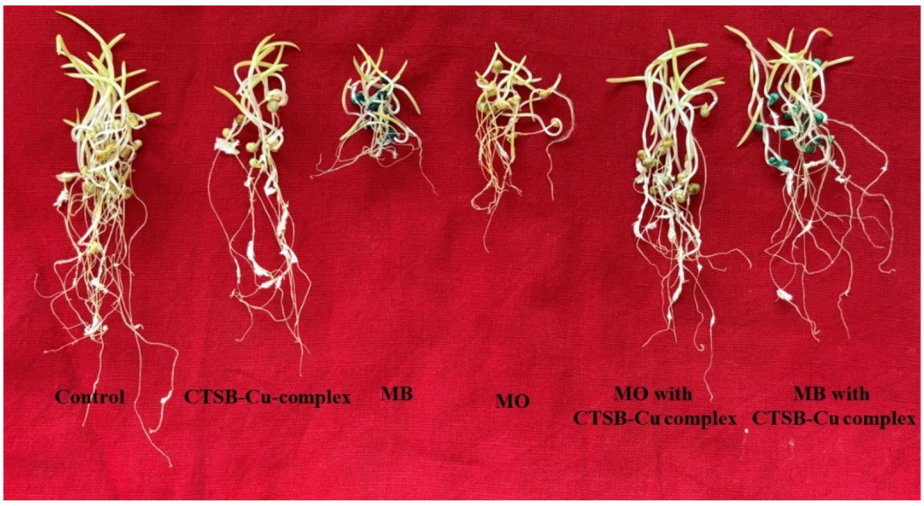

Fig. 12 Pearl millet seedlings treated with CTSB-Cu-complex, methylene blue, methyl orange (MO), MO with CTSB-Cu-complex and MB with CTSB-Cu-complex.

Table 5 Effect of metal complex on the seed germination, root length, and shoot length of pearl millet[a]

Treatments	Seed germination (%)	Exposure time (10 min.)		Exposure time (20 min.)	
		Shoot length (cm)	Root length (cm)	Shoot length (cm)	Root length (cm)
Control	80.00%	4.6–4.0 ± 0.32[a]	8.0–7.5 ± 0.39[a]	6.5–6.2 ± 0.27	8.8–8.6 ± 0.32[a]
Methylene blue (100 ppm)	50.00%	1.8–1.3 ± 0.56[a]	2.0–2.5 ± 0.46[a]	2.7–2.5 ± 0.48[a]	3.3–3.0 ± 0.42[a]
Methyl orange (100 ppm)	63.33%	2.3–2.0 ± 0.46[a]	2.8–3.2 ± 0.38[a]	2.8–2.6 ± 0.41[a]	3.8–3.5 ± 0.37[a]
Methylene blue (100 ppm) & CTSB-copper complex (150 PPM)	78.66%	4.3–3.9 ± 0.43[a]	7.9–6.8 ± 0.32[a]	6.0–5.8 ± 0.36[a]	8.0–7.5 ± 0.30[a]
Methyl orange (100 ppm) & CTSB-copper complex (150 PPM)	82.33%	4.5–4.3 ± 0.37[a]	7.8–7.0 ± 0.34[a]	6.6–5.9 ± 0.32[a]	8.3–8.0 ± 0.26[a]

[a] Duncan's test ($P \leq 0.05$) was utilized to determine the statistical significance. The resulting data were reported as mean values along with relevant standard deviation.

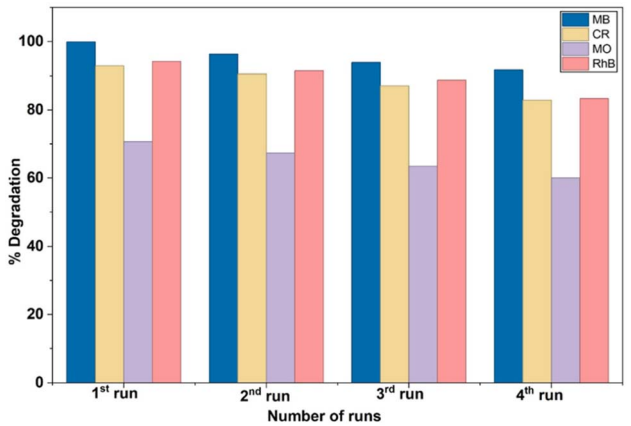

Fig. 13 Reusability of the CTSB-Cu-complex for the degradation of the MB, Cr, MO and RhB dyes.

The results indicated that the CTSB-copper complex mineralized dyes before affecting the germination and other physiological features (Table 5).

3.5. Reusability of the CTSB-copper complex

In environmentally benign methodology, recyclability and reusability of a catalyst is an utmost important parameter to evaluate its performance. Therefore, to examine the recyclability and reusability of the CTSB-copper complex, dye degradation experiments were performed under similar reaction conditions. Once the maximum degradation of dyes was achieved, the CTSB-copper complex was separated by filtration. The recovered CTSB-copper complex was collected and washed with water and ethanol, dried and reused directly in subsequent experiments for the degradation process of dyes. As shown in Fig. 13, the CTSB-copper complex could be recycled and successfully reused four times without substantial loss in degradation performance.

4. Conclusion

In this study, we reported the synthesis, characterization, antioxidant scavenging assay of coumarin thiazole-derived Schiff base (CTSB)-copper complex and their application for the catalytic degradation of methylene blue, methyl orange Congo red and rhodamine B dyes, along with the impact on pearl millet seed germination. The coumarin thiazole Schiff base (CTSB) ligand was synthesized from diethylamino salicylaldehyde and coumarin-thiazole-based amine in excellent yield using a facile synthetic procedure. The Schiff base CTSB provides a unique hetero-tridentate coordination environment around the copper ion by extending the π-conjugated system with multiple donor sites (O, N, and S). This combination significantly improves chelation and electron transfer, stabilizes the metal centre, and improves the effective light-absorbing capacity. The developed CTSB-copper complex showed outstanding catalytic activity for the rapid degradation of methylene blue and rhodamine B, achieving 99.89% and 94.22% within 35.0 seconds and 3.0 minutes at room temperature, respectively, under exposure to sunlight. Moreover, the reported complex degraded methyl orange and Congo red with efficiency of 70.65% and 92.88% within 12.0 minutes and 20.0 minutes, respectively, at room temperature under exposure to sunlight, whereas a similar percentage of degradation was obtained within 12.0 minutes and 4.0 minutes, respectively, when exposed to ultraviolet light. The CTSB-copper complex showed high antioxidant activity (90.59%) against DPPH assays recorded at 2.5 mg mL^{-1}, exhibiting its capacity to scavenge free radicals. Further, treatment with the CTSB-copper complex neutralizes the effect of methylene blue and methyl orange dyes on the percentage germination of hybrid pearl millet seeds (RHB-234 improved) and other physiological features. The present finding suggests that the CTSB-copper complex could be a valuable, sustainable tool for addressing challenges in agricultural and environmental remediation sectors. Along with several advantages shown in the present findings, it is crucial to improve the applicability of the Schiff base–copper complex for degradation of various categories of dyes.

Conflicts of interest

The authors declare that they have no known competing financial interests or personal relationships that could have appeared to influence the work reported in this paper.

Data availability

The data used in this study are included in the manuscript. Additional data or supplementary information (SI) can be provided upon reasonable request. Supplementary information is available. See DOI: https://doi.org/10.1039/d5ra08232c.

Acknowledgements

Neelam Sharma and R. S. are obliged to Manipal University Jaipur for providing the lab facility and infrastructures. Authors gratefully acknowledge the Central Analytical Facilities of Manipal University, Jaipur, for providing the UV-visible, FT-IR and fluorescence spectroscopy instruments.

References

1 T. Sinha and M. J. E. S. Ahmaruzzaman, *Environ. Sci. Pollut. Res.*, 2015, **22**(24), 20092–20100.
2 V. Mirkhani, S. Tangestaninejad, M. Moghadam, M. H. Habibi and A. Rostami-Vartooni, *J. Iran. Chem. Soc.*, 2009, **6**(3), 578–587.
3 J. S. Knapp, P. S. Newby and L. P. Reece, *Enzyme Microb. Technol.*, 1995, **17**(7), 664–668.
4 S. Sarnaik and P. Kanekar, *J. Appl. Bacteriol.*, 1995, **79**(4), 459–469.
5 J. B. Fathima, A. Pugazhendhi, M. Oves and R. Venis, *J. Mol. Liq.*, 2018, **260**, 1–8.
6 V. Selvaraj, T. S. Karthika, C. Mansiya and M. J. J. O. Alagar, *J. Mol. Struct.*, 2021, **1224**, 129195.
7 S. K. Sen, S. Raut, P. Bandyopadhyay and S. Raut, *Fungal Biol. Rev.*, 2016, **30**(3), 112–133.
8 M. Sudha, A. Saranya, G. Selvakumar and N. Sivakumar, *Int. J. Curr. Microbiol. Appl. Sci.*, 2014, **3**(2), 670–690.
9 E. A. Abdelrahman and R. M. Hegazey, *J. Inorg. Organomet. Polym. Mater.*, 2019, **29**(2), 346–358.
10 M. Manimohan, S. Pugalmani, K. Ravichandran and M. A. Sithique, *RSC adv.*, 2020, **10**(31), 18259–18279.
11 E. Rodríguez, M. A. Pickard and R. Vazquez-Duhalt, *Curr. Microbiol.*, 1999, **38**(1), 27–32.
12 M. T. Moreira, I. Mielgo, G. Feijoo and J. M. Lema, *Biotech. Lett.*, 2000, **22**(18), 1499–1503.
13 K. Itoh, Y. Kitade and C. Yatome, *Bull. Environ. Contam. Toxicol.*, 1998, **60**(5), 786–790.
14 R. Malav and S. Ray, *Inorg. Chim. Acta*, 2023, **551**, 121478.
15 A. M. Abu-Dief and I. M. Mohamed, Beni-suef uni, *J. basic appl. Sci.*, 2015, **4**(2), 119–133.
16 A. Xavier and N. Srividhya, IOSR J, *Appl. Chem.*, 2014, **7**(11), 06–15.
17 S. Swami, N. Sharma and R. Shrivastava, *Int. J. Environ. Anal. Chem.*, 2025, **105**(20), 1–15.
18 O. A. El-Gammal, F. S. Mohamed, G. N. Rezk and A. A. El-Bindary, *J. Mol. Liq.*, 2021, **326**, 115223.
19 B. S. Sail, V. H. Naik, M. R. Kamli and B. M. Prasanna, *J. Mol. Struct.*, 2023, **1277**, 134837.
20 A. Li, Y. H. Liu, L. Z. Yuan, Z. Y. Ma, C. L. Zhao, C. Z. Xie, W. G. Bao and J. Y. Xu, *J. Inorg. Biochem.*, 2015, **146**, 52–60.
21 S. Swami, N. Sharma, A. Agarwala, V. Shrivastava and R. Shrivastava, *Mater. Today: Proc.*, 2021, **43**, 2926–2932.
22 T. Ashraf, B. Ali, H. Qayyum, M. S. Haroone and G. Shabbir, *Inorg. Chem. Commun.*, 2023, **150**, 110449.
23 S. G. Alka, R. Kumar, P. Singh, N. Gandhi and P. Jain, *Results Chem.*, 2023, **5**, 100849.
24 S. Shekhar, A. M. Khan, S. Sharma, B. Sharma and A. Sarkar, *Emergent Mater*, 2022, **5**(2), 279–293.
25 A. Shafie and A. A. Ashour, *J. Inorg. Biochem.*, 2025, 112909.
26 M. Claudel, J. V. Schwarte and K. M. Fromm, *Chem*, 2020, **2**, 849–899.
27 G. Gasser and N. M. Nolte, *Curr. Opin. Chem. Biol.*, 2012, **16**, 84–91.
28 I. Kostova, *Curr. Med. Chem. Anti-Cancer Agents*, 2005, **5**(1), 29–46.
29 F. S. A. Rahman, S. K. Yusufzai, H. Osman and D. Mohamad, *J. Phys. Sci.*, 2016, **27**(1), 77–87.
30 M. Zabradnic, *The Production and Application of Fluorescent Brightening Agents*, John wiley and sons, New york, 1992.
31 R. O'Kennedy and R. D. Thornes, *Coumarins: Biology, Applications and Mode of Action*, John Wiley and Sons, New York, 1997, p. 348.
32 M. Maeda, *Laser Dyes*, Academic, New York, 1994.
33 S. Venkataraman, R. Meera, V. Ramachandran, P. Devi, A. Aruna, S. P. T. Parameswari and K. Nagarajan, *Inter. J. Pharm. Rev. Res.*, 2014, **4**, 25–32.
34 S. Cascioferro, B. Parrino, D. Carbone, D. Schillaci, E. Giovannetti, G. Cirrincione and P. Diana, *J. med. Chem.*, 2020, **63**(15), 7923–7956.
35 H. Wan, S. Habib, H. Liu and S. Mahmud, *Results Surf. Interf.*, 2024, **14**, 100194.
36 P. Mahadevi and S. Sumathi, *Results Chem.*, 2023, **6**, 101026.
37 L. J. Li, L. K. Yang, Z. K. Chen, Y. Y. Huang, B. Fu and J. L. Du, *Inorg. Chem. Commun.*, 2014, **50**, 62–64.
38 M. S. Refat, H. A. Saad, A. A. Gobouri, M. Alsawat, A. M. A. Adam and S. M. El-Megharbel, *J. Mol. Liq.*, 2022, **345**, 117140.
39 X. J. Hong, X. Liu, J. B. Zhang, C. L. Lin, X. Wu, Y. J. Ou, H. G. Jin and Y. P. Cai, *Cryst. Eng. Comm.*, 2014, **16**(34), 7926–7932.
40 M. Rana, R. Arif, F. I. Khan, V. Maurya, R. Singh, M. I. Faizan, S. Yasmeen, S. H. Dar, R. Alam, A. Sahu and T. Ahmad, Rashisuddin, *Bioorg. Chem.*, 2021, **108**, 104665.
41 B. Rani, A. Agarwala, D. Behera, V. P. Verma, A. P. Singh and R. Shrivastava, *Dyes Pigm.*, 2021, **194**, 109596.
42 R. Manjunath, M. Padmapriya, S. Pandey, R. Nayak, K. S. R. Pai and S. L. Gaonkar, *J. Mol. Struct.*, 2026, **1352**, 144465.
43 Ł. Czekański, S. K. Hoffmann, P. Barczyński, A. Gąsowska, R. Bregier-Jarzębowska, A. Zalewska, J. Goslar, M. Ratajczak-Sitarz and A. Katrusiak, *New J. Chem.*, 2016, **40**(12), 10526–10535.
44 M. Manimohan, S. Pugalmani, K. Ravichandran and M. A. Sithique, *RSC Adv.*, 2020, **10**(31), 18259–18279.
45 A. K. Abay, X. Chen and D.-H. Kuo, *New J. Chem.*, 2017, **41**(13), 5628–5638.
46 A. A. Kassem, H. N. Abdelhamid, D. M. Fouad and S. A. Ibrahim, *Micropor. Mesopor. Mat.*, 2020, **305**, 110340.